Available online at www.sciencedirect.com
SCIENCE DIRECT®
Bioorganic & Medicinal Chemistry Letters
ELSEVIER
Bioorganic & Medicinal Chemistry Letters 14 (2004) 1447–1454

HIV-1 integrase pharmacophore model derived from diverse classes of inhibitors

Gabriela Iurcu Mustata,[a,†] Alessandro Brigo[b] and James M. Briggs[a,*]

[a]*Department of Biology and Biochemistry, University of Houston, Houston, TX 77204-5001, USA*
[b]*Dipartimento di Scienze Farmaceutiche, Università degli Studi di Padova, 35131 Padova, Italy*

Received 29 September 2003; revised 9 January 2004; accepted 14 January 2004

Abstract—A three-dimensional pharmacophore model has been generated for HIV-1 integrase (HIV-1 IN) from known inhibitors. A dataset consisting of 26 inhibitors was selected on the basis of the information content of the structures and activity data as required by the CATALYST/HYPOGEN program. Our model was able to predict the activity of other known HIV-1 IN inhibitors not included in the model generation, and can be further used to identify structurally diverse compounds with desired biological activity by virtual screening.

1. Introduction

Human immunodeficiency virus type 1 is the etiological agent of acquired immunodeficiency syndrome (AIDS). HIV encodes three enzymes: reverse transcriptase, protease and integrase. Only the first two enzymes have been successfully exploited as targets for antiviral drugs. The emergence of strains resistant to currently available reverse transcriptase and protease inhibitors has led to the necessity to focus on new targets. An essential step in HIV replication is the integration of the transcribed double-stranded viral DNA into the host chromosomes which is carried out by HIV-1 integrase (IN).[2,3] Integration occurs in two consecutive reactions:[4] in the first step, termed 3′-processing, an activated water molecule attacks each 3′-end of the viral DNA removing a dinucleotide from each; in the second step, called 'strand transfer', each exposed viral DNA 3′-OH ribose is activated for nucleophilic attack on opposite strands of the host DNA, becoming covalently attached to them. Nucleophile activation occurs through the action of Mg^{2+} ions in the active site. To date, a number of classes of compounds have been identified to be active either against the 3′-processing or strand transfer,[5–13] but none of them have completed clinical trials because of their limited potency or high toxicity. In contrast to HIV-1 protease and reverse transcriptase, where a number of crystal structures of the enzyme–ligand complexes are available, HIV-1 IN is lacking the structural information that would allow clear derivation of the important three-dimensional arrangements and the essential functional groups needed by a compound to effectively interact with the enzyme. Only one crystal structure of HIV-1 IN with a bound inhibitor (5CITEP) in the active site is currently available.[14]

Despite the paucity of structural information at a molecular level about IN–inhibitor interactions, a considerable number of activity data for inhibitors that belong to diverse chemical classes is currently available. Several compounds such as dioxepinones,[5] quinones,[5] benzoic hydrazides,[7] thiazolothiazepines,[8] salicylpyrazolinones,[9] coumarins,[11] etc., have been reported to inhibit integrase's enzymatic activity at low micromolar concentrations. Pommier et al. have reported the development of pharmacophore models[15–18] derived from a series of HIV-1 IN inhibitors. These pharmacophore models were used to search the National Cancer Institute three-dimensional (3D) Structural Database and some of those compounds were found to inhibit both 3′-processing and strand transfer of IN at micromolar concentrations. Recently, a series of compounds representing a new class, typified by an aryl β-diketo motif (from the Merck laboratories), revealed very high activities and strong selectivity for the inhibition of the strand

Keywords: HIV-1 integrase; Inhibitor design; Pharmacophore model.
* Corresponding author. Tel.: +1-713-743-8366; fax: +1-713-743-8351; e-mail: jbriggs@uh.edu
† Present address: Emisphere Technologies, Inc., Tarrytown, NY 10591, USA.

0960-894X/$ - see front matter © 2004 Elsevier Ltd. All rights reserved.
doi:10.1016/j.bmcl.2004.01.027

transfer process.[10] Furthermore, a recent report[12] has shown that novel bioisosteric β-diketo acid analogues containing an 8-hydroxy-[1,6]-naphthyridine moiety inhibit HIV-1 integrase at comparable and even lower concentrations with respect to the Merck compounds.

In accordance with these recent results, we decided to exploit this wealth of information to develop a small molecule-derived pharmacophore model. The approach we are using here is to develop a pharmacophore model using the HYPOGEN module in CATALYST[1] which can be used to correlate the observed biological activities for a series of compounds with their chemical structures. We have included in our study the biological activity data of 26 compounds, which covers 5 orders of magnitude. These molecules were selected to span the range of activities from the most active compounds that are publicly available to almost completely inactive molecules.

Since there is no recent report on developing pharmacophore models using newly published inhibitors, the present study provides a hypothetical picture of the primary chemical features responsible for activity, and is expected to provide useful knowledge for developing new inhibitors targeted to HIV-1 integrase.

2. Pharmacophore generation and mapping

Over the last few years, a number of classes of HIV-1 IN inhibitors have been identified. We have collected a set of 431 molecules whose HIV-1 integrase activity data were taken from the literature. The biological dataset was divided into a training set (Table 1) and into a test set (Table 4). The training set consists of 26 structures and was selected by considering both structural diversity and wide coverage of the activity range (that is IC_{50} ranging from 0.04 μM (compound **11** in Table 1) to 1000 μM (compound **15** in Table 1)). The molecules from the training set were selected as a function of their activity against the strand transfer process without considering the selectivity of the molecules between 3′-processing and strand transfer. These molecules, whose activities span a range of 5 orders of magnitude, were selected based on the fact that each order of magnitude is represented by at least three compounds, including the most active and inactive ones. If two compounds had similar structures, they had to differ in activity by one order of magnitude to be included in our dataset. Otherwise, we selected only the most active one of the two. If two compounds were found to have similar activities, they had to be structurally distinct in order to be included. The structures of the 26HIV-1 IN inhibitors used in the training set are given in Table 1 along with their biological activities.

An uncertainty value of 3 was used for compound activity, representing the ratio between the upper range of biological activity for the compound and the actual activity. Uncertainty influences the first step, called the constructive phase, in the hypothesis generating process.[19] During this step, hypotheses that are common among the active compounds in the training set are generated. The activities (IC_{50}) against HIV-1 IN have been classified as follows: highly active ($IC_{50} \leq 10$ μM), moderately active (100 μM $> IC_{50} >$ 10 μM) and inactive ($IC_{50} \geq 100$ μM).

The compounds were built using CATALYST 2D–3D sketcher[1] and a representative family of conformations was generated for each molecule using the Poling algorithm[20] and the 'best conformational analysis' method. Conformations of all training set molecules were selected using an energy constraint of 20 kcal/mol or less above the local minimized structures. A maximum of 250 conformations of each molecule were generated to ensure maximum coverage of the conformational space, while conserving computer time.

An analysis of the training set revealed that five chemical features, that is, hydrogen-bond acceptor (HA), hydrogen-bond donor (HD), hydrophobic (HY), negative charge (NC) and ring aromatic (RA) could effectively map all of the critical chemical features.

The 'Best Compare/Fit'[1] procedure was then used in order to evaluate the geometry of the conformers of the compounds to test how well they fit the hypothesis. The fit value represents the quality of the mapping between the compound and the hypothesis; the better the overall superimposition of functional groups of the molecule to the appropriate features of the pharmacophore model, the higher the fit score.[21]

3. Pharmacophore hypothesis generation

The HypoGen module in CATALYST[1] performs a 'fixed cost' calculation, which represents the simple model that fits all data perfectly, and a 'null cost' calculation, which presumes that there is no relationship in the dataset and that the experimental activities are normally distributed around their average value. A meaningful pharmacophore hypothesis may result when the difference between these two values is large; a value of 40–60 bits for a pharmacophore hypothesis may suggest that it has 75–90% probability of correlating the data.[19] The total cost of any pharmacophore hypothesis should be close to the fixed cost to provide any useful models.

A set of 10 hypotheses was generated using the data from 26 training compounds (Table 1). The cost values, correlation coefficients (r), root-mean square (RMS) deviations, and pharmacophore features are listed in Table 2.

The first hypothesis (Hypo1) is the best pharmacophore hypothesis in this study, characterized by the highest cost difference (50), lowest RMS error (1.4) and the best correlation coefficient (0.85). The fixed cost, pharmacophore cost and null cost are 106, 132 and 182, respectively. From Table 2 we can see that all 10 hypotheses contain the hydrogen-bond donor feature (HD). Seven of the hypotheses have a hydrogen-bond acceptor feature (HA) and one hydrophobic (HY), whereas five of

Table 1. Training set molecules used to develop pharmacophore hypotheses for HIV-1 IN

Compd	Chemical structure	Class	ST IC_{50} (μM)
1	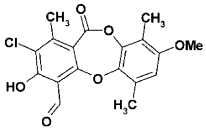	Dioxepinones[5]	2.1
2	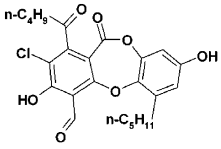	Dioxepinones[2,5]	33.6
3	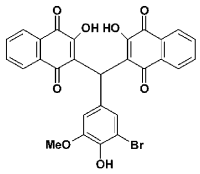	Quinones[6]	20
4	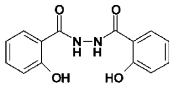	Benzoic hydrazides[7]	0.7
5	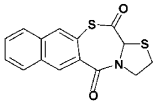	Thiazolothiazepines[8]	47
6	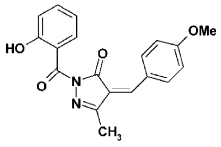	Salicylpyrazolinones[9]	0.6
7	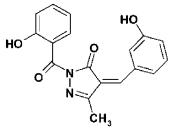	Salicylpyrazolinones[9]	7.4
8	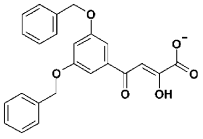	β-Diketo acids[10] (L-708,906)	0.059
9	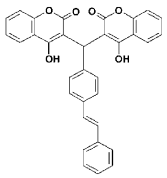	Coumarins[11]	3.7
10	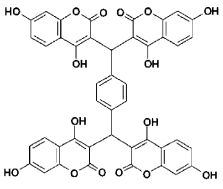	Coumarins[11]	0.33±0.30
11	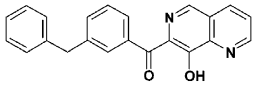	Naphtyridines[12]	0.04
12	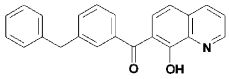	Quinolines[13]	0.37
13	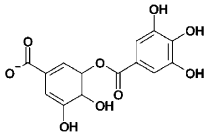	Depsides and depsidones[5]	0.6
14	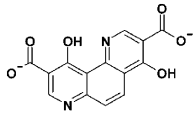	Depsides and depsidones[5]	6.1
15	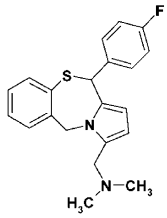	Thiazolothiazepines[8]	1000
16	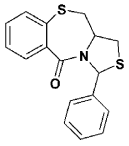	Thiazolothiazepines[8]	322
17	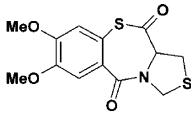	Thiazolothiazepines[8]	331
18	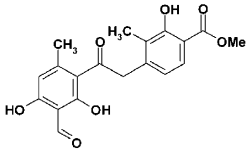	Dioxepinones[9]	123.0
19	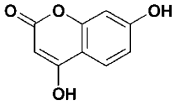	Coumarins[10]	325
20	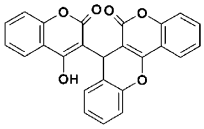	Coumarins[10]	122–163

(*continued on next page*)

Table 1 (*continued*)

Compd	Chemical structure	Class	ST IC_{50} (μM)
21	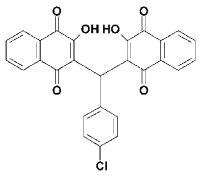	Quinones[6]	>100
22	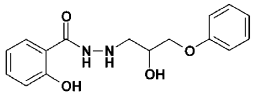	Benzoic hydrazides[7]	>200
23	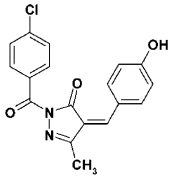	Salicyl-pyazolinones[9]	>293
24	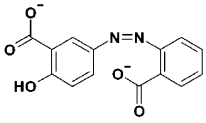	Depsides and depsidones[5]	224
25	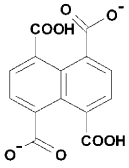	Depsides and depsidones[5]	182.2
26	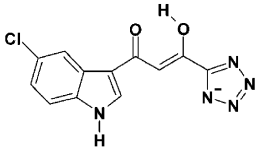	β-Diketo acids[14] (5CITEP)	>200

the hypotheses have one ring aromatic feature (RA). The top ranked hypothesis (Hypo1) contains four features: 2 hydrogen-bond acceptor groups, one hydrogen-bond donor and one hydrophobic group (Fig. 1).

The pharmacophore cost is well below the null cost and closer to the fixed cost, which indicates that the correlation is not fortuitously obtained. Figure 2 shows the top-ranked hypothesis, named Hypo1, aligned with the highest active compounds (compound **8** (IC_{50} = 0.059 μM) and compound **11** (IC_{50} = 0.04 μM)) of the training set molecules.

Hypothesis 1, identified as the best model, was used to estimate the activities of the training set compounds. As we have mentioned, all compounds in this study were classified by their activity as highly active ($IC_{50} \leq 10$ μM, +++), moderately active (100 μM > IC_{50} > 10 μM, ++), and inactive ($IC_{50} \geq 100$ μM, +).

Table 3 shows the actual and estimated inhibitory

Table 2. Results of pharmacophore hypotheses generated by CATALYST/HYPOGEN[1]

Hypothesis No.[a]	Total cost	Cost difference (null cost–total cost)	RMS	Correlation	Features[b]
1	132	50	1.4	0.85	HA, HA, HD, HY
2	138	44	1.5	0.82	HA, HA, HD, HY
3	139	43	1.6	0.81	HA, HD, HY
4	139	43	1.6	0.80	HA, HD, HY, RA
5	140	42	1.6	0.80	HA, HD, HY, RA
6	140	42	1.6	0.80	HA, HD, HY
7	140	42	1.6	0.80	HA, HD, HY, NC
8	141	41	1.6	0.81	HD, RA
9	141	41	1.6	0.80	HD, RA, RA
10	142	40	1.6	0.81	HD, RA

[a] Null cost = 182. Fixed cost = 106. Configuration cost = 18. All cost units are in bits.
[b] HA, hydrogen-bond acceptor; HD, hydrogen-bond donor; HY, hydrophobic; RA, ring aromatic; NC, negative charge.

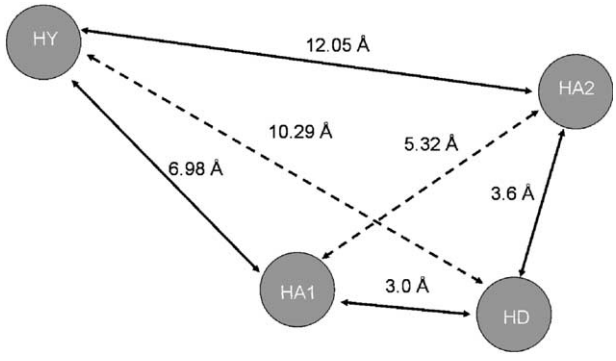

Figure 1. Two-dimensional representation of the top-ranked hypothesis (Hypo1). HA represents the hydrogen-bond acceptor feature; HY, hydrophobic and HD, hydrogen-bond donor.

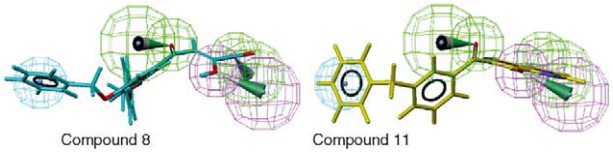

Figure 2. Mapping of the two most active compounds from the training set (compounds **8** and **11** in Table 1), on the selected pharmacophore hypothesis (Hypo1). Pharmacophore features are color-coded (green represents the hydrogen-bond acceptor feature (HA), blue represents the hydrophobic feature (HY) and violet represents the hydrogen-bond donor feature (HD).

activities of the 26 molecules from the training set, based on the pharmacophore model hypothesis, Hypo1. All highly active compounds were predicted correctly, with the exception of compound **1** (that is its activity was estimated as moderately active). The three moderately active compounds were well predicted, and half of the inactive compounds were correctly predicted to be inactive, the other half being predicted as moderately active. There is only one compound, categorized as

Table 3. Experimental biological data (IC_{50}) and estimated activity (IC_{50}) of training set molecules based on the top ranked hypothesis (Hypo1)

Compd	Actual IC_{50} (μM)	Estimated IC_{50} (μM)	Error[a]	Fit value[b]	Mapped feature				Activity scale[c]	Estimated activity scale
					HA1	HA2	HD	HY		
1	2.1	40	+19	3.8	+	–	–	+	+ + +	+ +
2	33.6	27	−1.2	4.0	+	+	–	+	+ +	+ +
3	20	30	+1.5	3.9	+	–	–	+	+ +	+ +
4	0.7	1.3	+1.8	5.3	+	+	+	–	+ + +	+ + +
5	47	68	+1.4	3.6	+	+	–	–	+ +	+ +
6	0.6	2.5	+4.2	5.0	+	–	+	+	+ + +	+ + +
7	7.4	6.9	−1.1	4.6	+	–	+	+	+ + +	+ + +
8	0.06	0.031	−2	6.9	+	+	+	+	+ + +	+ + +
9	3.7	3.7	+1	4.9	+	+	–	+	+ + +	+ + +
10	0.33	0.48	+1.5	5.7	+	+	–	+	+ + +	+ + +
11	0.04	0.6	+15	5.6	+	–	+	+	+ + +	+ + +
12	0.37	0.62	+1.7	5.6	+	–	+	+	+ + +	+ + +
13	0.6	2.2	+3.7	5.1	+	+	+	–	+ + +	+ + +
14	6.1	39	+6.5	3.8	+	–	+	–	+ + +	+ +
15	1000	2800	+2.8	2.0	–	–	–	+	+	+
16	322	210	−1.5	3.1	+	+	–	–	+	+
17	331	100	−3.3	3.4	+	+	–	–	+	+
18	123	31	−3.9	3.9	–	+	–	+	+	+ +
19	325	130	−2.5	3.3	+	+	–	–	+	+
20	122	59	−2.1	3.6	+	+	–	–	+	+ +
21	100	30	−3.4	3.9	+	–	–	+	+	+ +
22	200	5.5	−36	4.7	+	+	+	–	+	+ + +
23	293	29	−10	4.0	–	+	–	+	+	+ +
24	224	38	−5.9	3.8	+	–	+	–	+	+ +
25	180	2300	+13	2.1	+	+	–	–	+	+
26	200	40	−5	3.8	+	–	–	+	+	+ +

[a] + Indicates that the estimated IC_{50} is higher than the actual IC_{50}; − indicates that the estimated IC_{50} is lower than the actual IC_{50}; a value of 1 indicates that estimated IC_{50} is equal to the actual IC_{50}.
[b] Fit value indicates how well the features in the pharmacophore overlap the chemical features in the molecule.
[c] HIV-1 IN activity scale: + + +, $IC_{50} \leq 10$ μM (highly active); + +, $100 > IC_{50} > 10$ μM (moderately active); +, $IC_{50} \geq 100$ μM (inactive).

inactive, for which the activity was estimated to be highly active (compound **22** in Tables 1 and 3). However, the activity of compound **4**, which is part of the same class, was predicted correctly. The discrepancy between the actual and estimated activity observed for compound **22** might be an artifact of the program that is using the larger number of degrees of freedom of this molecule to better fit the pharmacophore model. Interestingly, all highly active compounds mapped the first hydrogen-bond acceptor feature (HA1), and, with few exceptions, they also mapped the hydrophobic feature, revealing a good correlation between the high fit values and the predicted activity (see Table 3).

These observations provide a compelling indication that these two features may be responsible for high activity and could be taken advantage of in the design of novel HIV-1 IN inhibitors.

4. Validation of the pharmacophore model generated from HIV-1 IN inhibitors

In order to validate our model, we have used a test set of fourteen highly active molecules,[10,12,22,23] including the most active of the recently published azido-containing HIV-1 IN inhibitors[24] (Table 4). All test molecules were built, minimized and conformers were generated in a similar way as the training set compounds. Hypo1 was regressed against the compounds of the test set and a score of 98% was achieved.

The test molecules were mapped onto the pharmacophore hypothesis and the experimental biological data versus estimated activities are shown in Table 5. All fourteen molecules were predicted as highly active, in perfect agreement with the actual biological data. All of the test compounds fitted the hydrogen-bond donor feature and the first hydrogen-bond acceptor feature. This is, again, an indication that these features might be essential for high binding affinity. Two of the test set molecules (i.e., azido-containing inhibitors; compounds **11** and **13** in Table 4) did not map the hydrophobic feature, while only three molecules of the test set (i.e., compounds **2**, **3** and **6**) did not fit the second hydrogen-bond acceptor feature.

One of the most active molecules from the test set (compound **2** in Table 4) was selected to show the mapping of this compound on the selected pharmacophore hypothesis Hypo1 (Fig. 3).

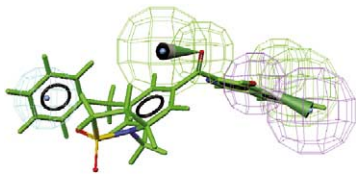

Figure 3. Mapping of the most active molecule from the test set (compound **2** in Table 4). Pharmacophore features are color-coded (green represents the hydrogen-bond acceptor feature (HA), blue represents the hydrophobic feature (HY) and violet represents the hydrogen-bond donor feature (HD).

Table 4. Chemical structures of the molecules forming the test set

Compd	Chemical structure	Class	IC_{50} (μM)
1	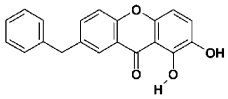	Xanthen-9-ones[12]	0.60 ST
2	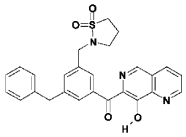	Naphtyridines[12]	0.01 ST
3	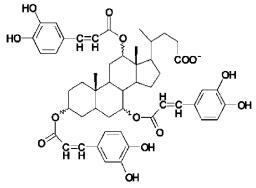	Cholic acid derivatives[22] (3,7,12,-tricaffeoyl-cholic acid)	0.97 (3′-processing) 0.75 (disintegration)
4	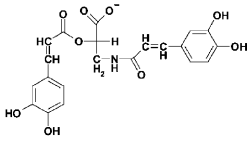	Succinic acids[22]	0.37 (3′-processing) 0.19 (disintegration)
5	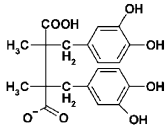	Succinic acids[22]	0.23 (3′-processing) 4.32 (disintegration)
6	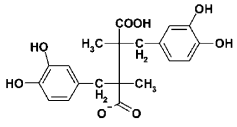	Succinic acids[22]	0.44 (3′-processing) 2.78 (disintegration)
	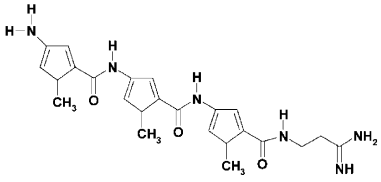 Distamycin		
7	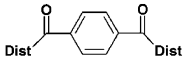	Bisdistamycins[23] Dist = Distamycin	0.09 ± 0.01 ST
8	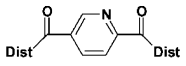	Bisdistamycins[23] Dist = Distamycin	0.1 ± 0.03 ST
Z =	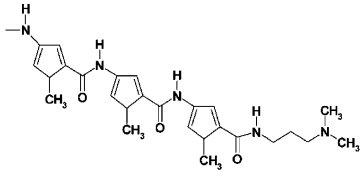		

(*continued on next page*)

Table 4 (*continued*)

Compd	Chemical structure	Class	IC_{50} (μM)
9	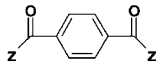	Lexitropsins[23]	0.07 ± 0.02 ST
10	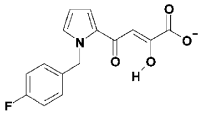	β-Diketo acids[10] (L-731,988)	0.126 ST
11	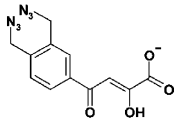	Azido-β-diketo acids[24]	0.26 ST
12	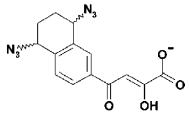	Azido-β-diketo acids[24]	0.32 ST
13	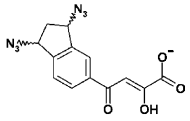	Azido-β-diketo acids[24]	0.36 ST
14	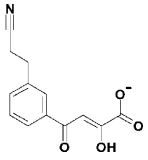	Azido-β-diketo acids[24]	1.5 ST

Table 5. Experimental biological data (IC_{50}) for IN inhibition and the estimated activity (IC_{50}) of the test set molecules based on the top ranked hypothesis (Hypo1)

Compd	Actual IC_{50} (μM)	Estimated IC_{50} (μM) based on Hypo1	Error[a]	Fit value[b]	Mapped feature				Activity scale[c]	Estimated activity scale
					HA1	HA2	HD	HY		
1	0.6	0.31	−2	6.5	+	+	+	+	+ + +	+ + +
2	0.01	0.1	8.9	6	+	—	+	+	+ + +	+ + +
3	0.97	0.81	−1.2	5.9	+	—	+	+	+ + +	+ + +
4	0.37	0.13	−2.9	7.2	+	+	+	+	+ + +	+ + +
5	0.23	0.84	3.7	7.1	+	+	+	+	+ + +	+ + +
6	0.44	1.7	3.9	5.9	+	—	+	+	+ + +	+ + +
7	0.09	0.11	1.2	6.2	+	+	+	+	+ + +	+ + +
8	0.1	0.12	1.2	6.6	+	+	+	+	+ + +	+ + +
9	0.07	0.11	1.6	6.4	+	+	+	+	+ + +	+ + +
10	0.13	0.15	1.2	6.7	+	+	+	+	+ + +	+ + +
11	0.26	0.16	−1.7	5.9	+	+	+	—	+ + +	+ + +
12	0.32	0.12	−2.6	6.5	+	+	+	+	+ + +	+ + +
13	0.36	0.29	−1.3	5.9	+	+	+	—	+ + +	+ + +
14	1.5	0.16	−9.3	6.1	+	+	+	+	+ + +	+ + +

[a] + Indicates that the estimated IC_{50} is higher than the actual IC_{50}; – indicates that the estimated IC_{50} is lower than the actual IC_{50}; a value of 1 indicates that estimated IC_{50} is equal to the actual IC_{50}.
[b] Fit value indicates how well the features in the pharmacophore overlap the chemical features in the molecule.
[c] HIV-1 IN activity scale: + + +, $IC_{50} \leq 10$ μM (highly active); + +, $100 > IC_{50} > 10$ μM (moderately active); +, $IC_{50} \geq 100$ μM (inactive).

This validation provides additional confidence in the proposed pharmacophore model. The utility of our pharmacophore is shown by the fact that the model elaborated within this study was able to accurately predict known inhibitors, including the recently published azido-containing HIV-1 IN inhibitors.[24] The mapping information based on the pharmacophore model we developed is now being taken advantage of in the identification of novel lead compounds with improved inhibitory activity through 3-D database searches.

Acknowledgements

This work was supported by the NIH Program on Structural Biology of AIDS Related Proteins (GM56553). Gratitude is expressed to Accelrys, Inc. (http://www.accelrys.com) for making the software available to us through the Institute for Molecular Design at the University of Houston. Supercomputer time for this project was granted by NRAC and made available on facilities at the University of Texas.

References and notes

1. CATALYST 4.6; Accelrys, Inc., San Diego, CA, 2001, http://www.accelrys.com
2. Asante-Appiah, E.; Skalka, A. M. *Antiviral Res*. **1997**, *36*, 139.
3. Hindmarsh, P.; Leis, J. *Microbiol. Mol. Biol. Rev*. **1999**, *63*, 836.
4. Brown, P. O.; Coffin, J. M.; Hughes, S. H.; Varmus, H. E. *Retroviruses*; Cold Spring Harbor Lab. Press: Plainview, New York, 1997; 161.
5. Neamati, N.; Hong, H.; Mazumder, A.; Wang, S.; Sunder, S.; Nicklaus, M. C.; Milne, G. W.; Proksa, B.; Pommier, Y. *J. Med. Chem*. **1997**, *40*, 942.
6. Mazumder, A.; Wang, S.; Neamati, N.; Nicklaus, M.; Sunder, S.; Chen, J.; Milne, G. W.; Rice, W. G.; Burke, T. R., Jr.; Pommier, Y. *J. Med. Chem*. **1996**, *39*, 2472.
7. Zhao, H.; Neamati, N.; Sunder, S.; Hong, H.; Wang, S.; Milne, G. W.; Pommier, Y.; Burke, T. R., Jr. *J. Med. Chem*. **1997**, *40*, 937.
8. Neamati, N.; Turpin, J. A.; Winslow, H. E.; Christensen, J. L.; Williamson, K.; Orr, A.; Rice, W. G.; Pommier, Y.; Garofalo, A.; Brizzi, A.; Campiani, G.; Fiorini, I.; Nacci, V. *J. Med. Chem*. **1999**, *42*, 3334.
9. Neamati, N.; Hong, H.; Owen, J. M.; Sunder, S.; Winslow, H. E.; Christensen, J. L.; Zhao, H.; Burke, T. R., Jr.; Milne, G. W.; Pommier, Y. *J. Med. Chem*. **1998**, *41*, 3202.
10. Hazuda, D. J.; Felock, P.; Witmer, M.; Wolfe, A.; Stillmock, K.; Grobler, J. A.; Espeseth, A.; Gabryelski, L.; Schleif, W.; Blau, C.; Miller, M. D. *Science* **2000**, *287*, 646.
11. Zhao, H.; Neamati, N.; Hong, H.; Mazumder, A.; Wang, S.; Sunder, S.; Milne, G. W.; Pommier, Y.; Burke, T. R., Jr. *J. Med. Chem*. **1997**, *40*, 242.
12. Zhuang, L.; Wai, J. S.; Embrey, M. W.; Fisher, T. E.; Egbertson, M. S.; Payne, L. S.; Guare, J. P., Jr.; Vacca, J. P.; Hazuda, D. J.; Felock, P. J.; Wolfe, A. L.; Stillmock, K. A.; Witmer, M. V.; Moyer, G.; Schleif, W. A.; Gabryelski, L. J.; Leonard, Y. M.; Lynch, J. J., Jr.; Michelson, S. R.; Young, S. D. *J. Med. Chem*. **2003**, *46*, 453.
13. Mekouar, K.; Mouscadet, J. F.; Desmaele, D.; Subra, F.; Leh, H.; Savoure, D.; Auclair, C.; d'Angelo, J. *J. Med. Chem*. **1998**, *41*, 2846.
14. Goldgur, Y.; Craigie, R.; Cohen, G. H.; Fujiwara, T.; Yoshinaga, T.; Fujishita, T.; Sugimoto, H.; Endo, T.; Murai, H.; Davies, D. R. *Proc. Natl. Acad. Sci. U.S.A*. **1999**, *96*, 13040.
15. Nicklaus, M. C.; Neamati, N.; Hong, H.; Mazumder, A.; Sunder, S.; Chen, J.; Milne, G. W.; Pommier, Y. *J. Med. Chem*. **1997**, *40*, 920.
16. Hong, H.; Neamati, N.; Wang, S.; Nicklaus, M. C.; Mazumder, A.; Zhao, H.; Burke, T. R., Jr.; Pommier, Y.; Milne, G. W. *J. Med. Chem*. **1997**, *40*, 930.
17. Hong, H.; Neamati, N.; Winslow, H. E.; Christensen, J. L.; Orr, A.; Pommier, Y.; Milne, G. W. *Antivir. Chem. Chemother*. **1998**, *9*, 461.
18. Neamati, N.; Hong, H.; Sunder, S.; Milne, G. W.; Pommier, Y. *Mol. Pharmacol*. **1997**, *52*, 1041.
19. Güner, O. F. In *Pharmacophore Perception, Development, and Use in Drug Design*; Ed.; International University Line: La Jolla, California, 2000, pp 173–188
20. Smellie, A.; Teig, S.; Towbin, P. *J. Comp. Chem*. **1994**, *16*, 171.
21. Barnum, D.; Greene, J.; Smellie, A.; Sprague, P. *J. Chem. Inf. Comput. Sci*. **1996**, *36*, 563.
22. Reinke, R. A.; King, P. J.; Victoria, J. G.; McDougall, B. R.; Ma, G.; Mao, Y.; Reinecke, M. G.; Robinson, W. E., Jr. *J. Med. Chem*. **2002**, *45*, 3669.
23. Neamati, N.; Mazumder, A.; Sunder, S.; Owen, J. M.; Tandon, M.; Lown, J. W.; Pommier, Y. *Mol. Pharmacol*. **1998**, *54*, 280.
24. Zhang, X.; Pais, G. C.; Svarovskaia, E. S.; Marchand, C.; Johnson, A. A.; Karki, R. G.; Nicklaus, M. C.; Pathak, V. K.; Pommier, Y.; Burke, T. R. *Bioorg. Med. Chem. Lett*. **2003**, *13*, 1215.